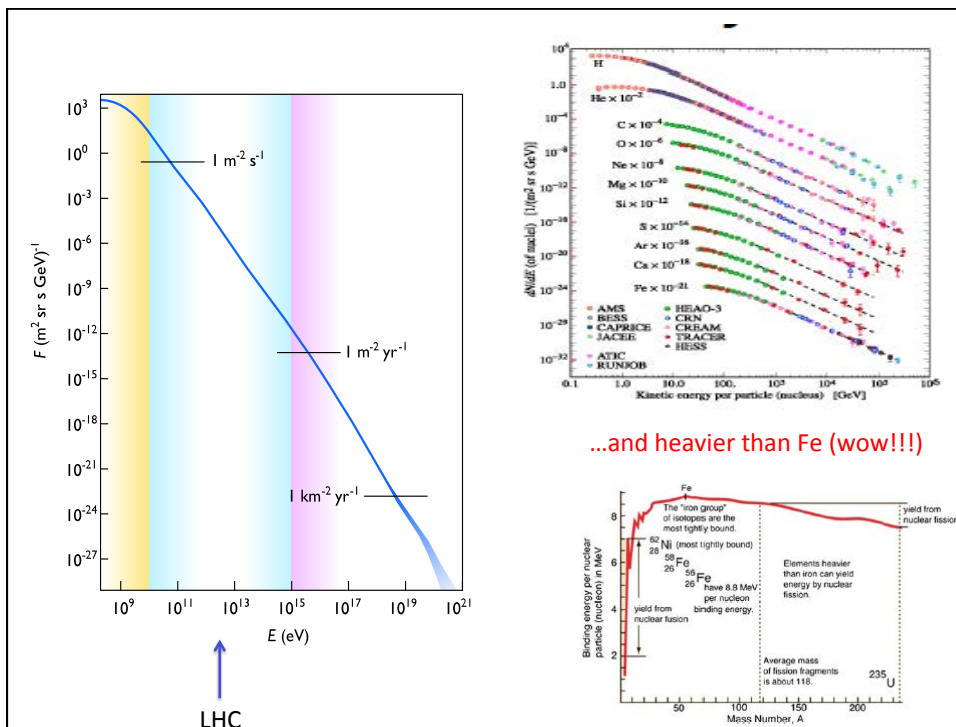


Multimessenger Astroparticle Physics

Alessandro De Angelis
 Univ. UD/PD, INFN/INAF Padova & LIP/IST Lisboa

3. Astrophysical Mechanisms of Particle Acceleration



...and heavier than Fe (wow!!!)

Multimessenger astrophysics

Several messengers can be used to study the properties of emitters (and btw particle physics)

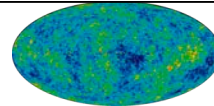
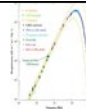
- **Charged cosmic rays.** The more abundant, but they don't point to the sources (astronomy with charged cosmic rays is almost impossible)
- **Gamma rays.** They are suppressed with respect to protons by a factor 1000-10000
- **Neutrinos.** Difficult to detect, small X-section
- **Gravitational waves.** Recent.

$$\frac{R_L}{1\text{kpc}} \simeq \frac{E/1\text{EeV}}{B/1\mu\text{G}}$$

3

Thermal radiation: Black Body Spectrum

Cosmic Microwave Background: 2.7 K



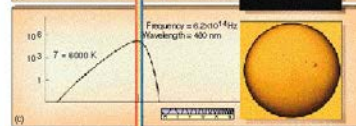
A Galactic gas cloud called Rho Ophiuchi: 60 K



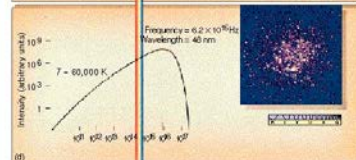
Dim star near the center of the Orion Nebula: 600 K



the Sun: 6000 K



Cluster of very bright stars, Omega Centauri, as observed from the space: 60,000 K

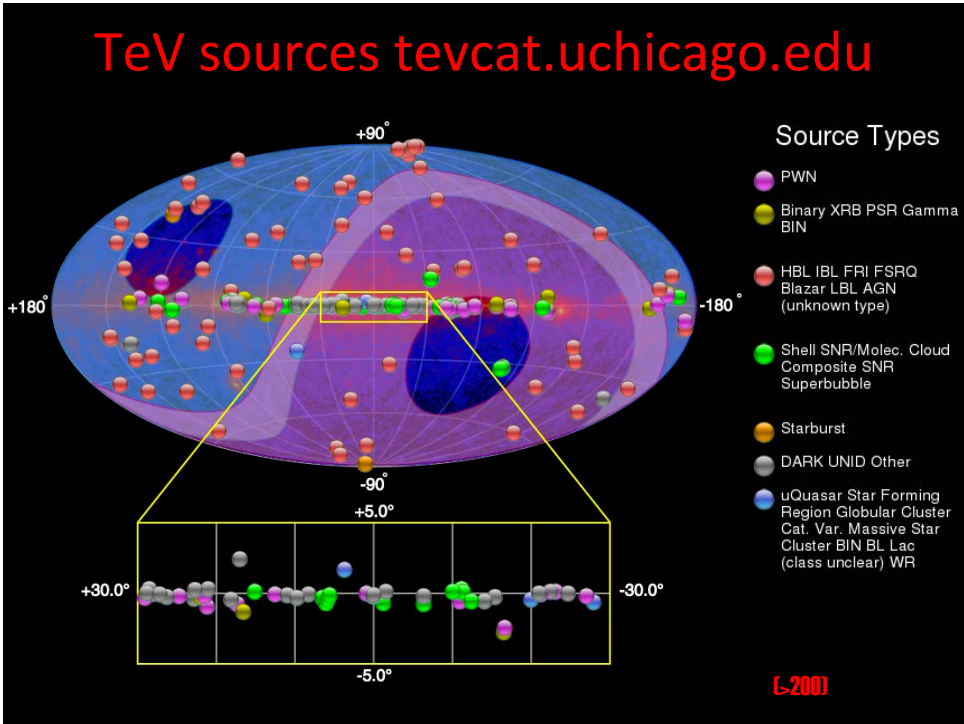


Accretion Disks can reach temperatures >> 10⁵ K



But this is still ~1 keV, in the X-Ray band!

4

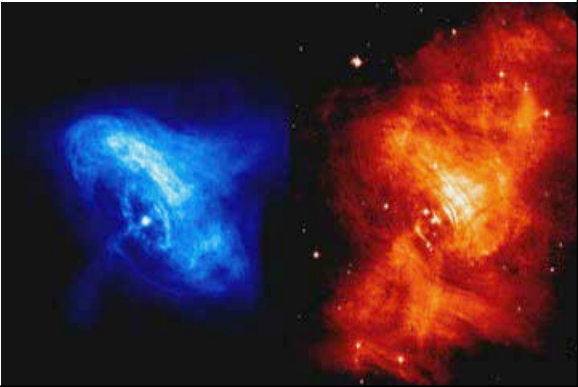


How does acceleration happen? Zwicky's conjecture:

1. Heavy enough stars collapse at the end of their lives into super-novae
2. Implosions produce explosions of cosmic rays
3. They leave behind neutron stars



(1934)

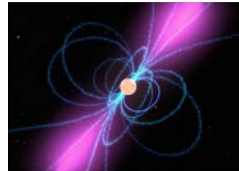


Examples of known extreme environments

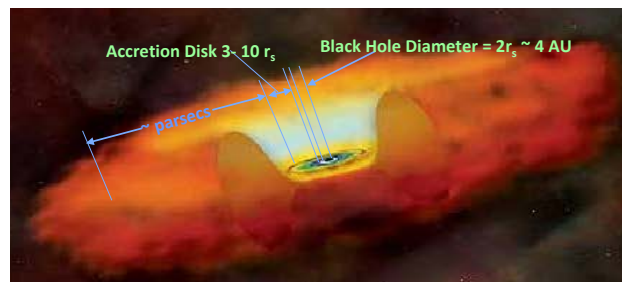
GRB



SuperNova Remnants
Pulsars



Active Galactic
Nuclei



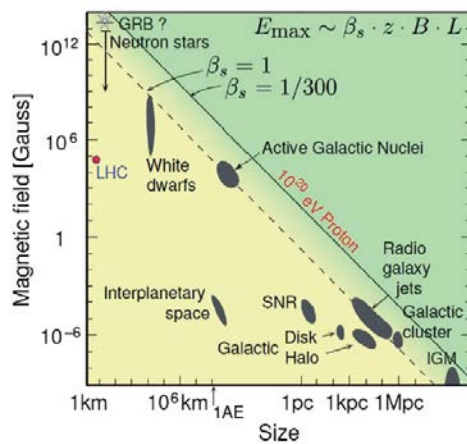
Possible sources of cosmic ray acceleration require

Magnetic field & dimensions
sufficient to contain the accelerating
particles.

Strong fields with large-scale
structure (astrophysical shocks)

$$E_{\text{max}} = \text{Eff} \times Z \times (B/1\mu\text{G}) (R/1 \text{ kpc})$$

- ISM-SN: (Lagage&Cesarsky, 1983)
- Wind-SN: (Biermann, 1993)
- AGN radio-lobes: (Rachen&Biermann,1993)
- AGN Jets or cocoon: (Norman et al.,1995)
- GRB: (Meszaros&Rees, 1992,1994)
- Neutron stars: (Bednarek&Protheroe,2002)
- Pulsar wind shock: (Berezhko, 1994)



Hillas, 1984

What is the physical mechanism?

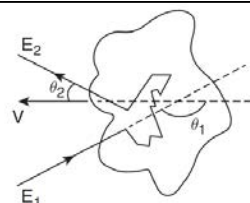


A. De Angelis



Acceleration Mechanism

Fermi Mechanism



Let us suppose (see Fig.10.4) that a charged particle with energy E_1 (velocity v) in the “laboratory” frame is scattering against a moving boundary between regions of different density (a partially ionized gas cloud). Due to the chaotic magnetic fields generated by its charged particles, the cloud will act as a massive scatterer. Let the cloud have a velocity $\beta = V/c$, and let θ_1 and θ_2 be the angles between, respectively, the initial and final particle momentum and the cloud velocity. Let us define $\gamma = 1/\sqrt{1 - \beta^2}$.

The energy of the particle E_1^* (supposed relativistic) in the cloud reference frame is given by (neglecting the particle mass with respect to its kinetic energy):

$$E_1^* \simeq \gamma E_1 (1 - \beta \cos \theta_1).$$

The cloud has an effective mass much larger than the particle’s mass, and thus it acts as a “magnetic mirror” in the collision. In the cloud reference frame $E_2^* = E_1^*$ (collision onto a wall), and in the laboratory frame the energy of the particle after the collision is:

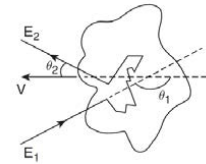
$$E_2 \simeq \gamma E_2^* (1 + \beta \cos \theta_2^*) = \gamma^2 E_1 (1 - \beta \cos \theta_1) (1 + \beta \cos \theta_2^*).$$

Thus the relative energy change is given by:

$$\frac{\Delta E}{E} = \frac{1 - \beta \cos \theta_1 + \beta \cos \theta_2^* - \beta^2 \cos \theta_1 \cos \theta_2^*}{1 - \beta^2} - 1$$

2nd order Fermi Mechanism

$$\frac{\Delta E}{E} = \frac{1 - \beta \cos \theta_1 + \beta \cos \theta_2^* - \beta^2 \cos \theta_1 \cos \theta_2^*}{1 - \beta^2} - 1.$$



The collision is the result of a large number of individual scatterings suffered by the particle inside the cloud, so the output angle in the c.m. is basically random. Then

$$\langle \cos \theta_2^* \rangle = 0.$$

The probability P to have a collision between a cosmic ray and the cloud is not constant as a function of the relative angle θ_1 ; it is rather proportional to their relative velocity (it is more probable that a particle hits a cloud that is coming against it, than a cloud that it is running away from it):

$$P \propto (v - V \cos \theta_1) \simeq (1 - \beta \cos \theta_1)$$

and thus

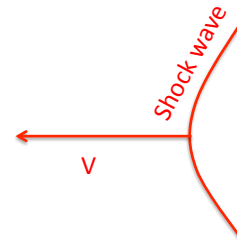
$$\langle \cos \theta_1 \rangle \simeq \frac{\int_{-1}^1 \cos \theta_1 (1 - \beta \cos \theta_1) d \cos \theta_1}{\int_{-1}^1 (1 - \beta \cos \theta_1) d \cos \theta_1} = -\frac{\beta}{3}. \quad (10.3)$$

The energy after the collision increases then in average by a factor

$$\left\langle \frac{\Delta E}{E} \right\rangle \simeq \frac{1 - \beta \langle \cos \theta_1 \rangle}{1 - \beta^2} - 1 \simeq \frac{1 + \beta^2/3}{1 - \beta^2} - 1 \simeq \frac{4}{3} \beta^2. \quad (10.4)$$

This mechanism is known as the second-order Fermi acceleration mechanism. It is not very effective, since the energy gain per collision is quadratic in the cloud velocity, and the random velocities of interstellar clouds in the Galaxy are very small, $\beta \sim 10^{-4}$; also the diffusion velocities directly measured, for example, in the observations of supernova remnants (see Fig. 10.5), are small ($\beta \sim 10^{-3} - 10^{-2}$).

Can we go to 1st order?

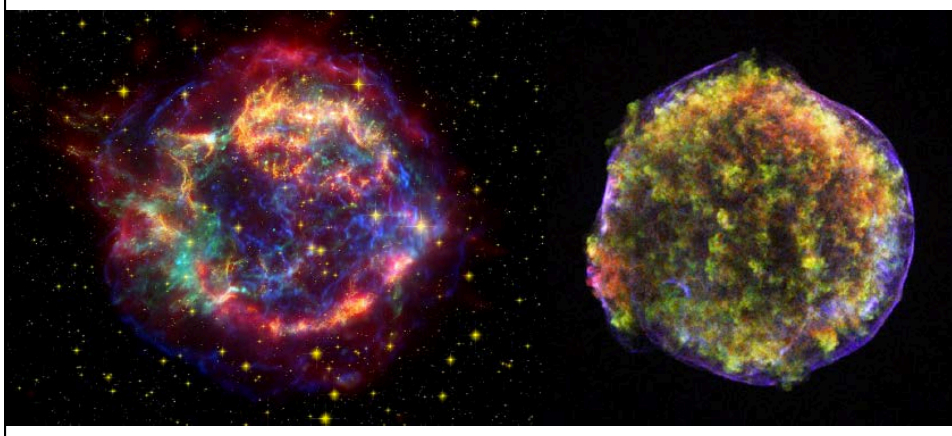


- **First-order Fermi Mechanism (Diffusive Shock Acceleration)**

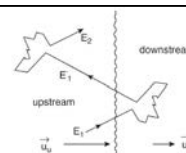
- $O(u/c)$ term gets lost in integral over angles in the 2nd order mechanism —we could retrieve this if we could arrange to have mostly head-on scatters
- Consider shock wave as sketched above
 - high-energy particles will scatter so that their distribution is isotropic in the rest frame of the gas
 - There is a preferred direction in the expansion
 => crossing shock **in either direction** produces head-on collision on average

Cas A (1680?); Tycho Supernova (SN 1572)

Shock front seen in high-energy electrons
 "Stripes" may signal presence of high-energy protons
 $v \sim c/100$



1st order Fermi mechanism (formal)



A shock wave creates a high-density region propagating with a locally plane wave front, acting like a piston. A shocked gas region runs ahead of the advancing piston into the interstellar medium. We assume that there is an abrupt discontinuity between two regions of fluid flow, and in the undisturbed region ahead of the shock wave, the gas is at rest. In the reference frame of the shock front, the medium ahead (upstream) runs into the shock itself with a velocity \mathbf{u}_u , while the shocked gas (downstream) moves away with a velocity \mathbf{u}_d (Fig. 10.6); according to the kinetic theory of gases, in a supersonic shock propagating through a monoatomic gas $|u_u| \sim 4|u_d|$. In the laboratory system, a particle coming from upstream to downstream meets in a head-on collision a high-density magnetized gas. The particle inverts the direction of the component of its initial velocity parallel to the shock front direction, crosses the shock front itself, and scatters with the gas upstream; it can bounce again and again within such a pair of parallel magnetic mirrors. Note that, although the system is equivalent from the point of view of the dynamics of the bouncing particle to a pair of mirrors approaching with a net relative velocity $V = |\mathbf{u}_u - \mathbf{u}_d|$, the two mirrors do not actually approach, since the molecules acting as mirrors belong for different rebounces to different regions of the gas, and the distance is approximately constant if the diffusion velocity does not vary.

If we put ourselves in the frame of reference of one of the clouds (upstream or downstream), each bound-rebound cycle is equivalent from the point of view of the energy gain to a collision in the laboratory with a head-on component into a cloud moving with speed V (see Fig. 10.4). Being the target gas coherently moving, the component of the velocity of the particle perpendicular to the direction of propagation of the shock wave will have a negligible change, while the component parallel to the direction itself will be inverted. If we call θ the angle between the (fixed) direction of the expansion and the direction of the incident particle, with the same convention as in Fig. 10.4, Eq. 10.2 becomes

$$\frac{\Delta E}{E} \simeq -2\beta \cos \theta, \quad (10.5)$$

$$\frac{\Delta E}{E} \simeq -2\beta \cos \theta$$

the angle θ between the particle initial velocity and the magnetic mirror being now constrained to the specific geometry: $-1 \leq \cos \theta \leq 0$. The probability of crossing the wave front is proportional to $-\cos \theta$, and Eq. 10.3 becomes:

$$\langle \cos \theta \rangle \simeq \frac{\int_{-1}^0 -\cos^2 \theta d \cos \theta}{\int_{-1}^0 -\cos \theta d \cos \theta} = -\frac{2}{3}. \quad (10.6)$$

The average energy gain for each bound-rebound cycle is:

$$\left\langle \frac{\Delta E}{E} \right\rangle \simeq -2\beta \langle \cos \theta \rangle \simeq \frac{4}{3}\beta \equiv \epsilon. \quad (10.7)$$

After n cycles the energy of the particle is:

$$E_n = E_0(1 + \epsilon)^n \quad (10.8)$$

i.e., the number of cycles needed to a particle to attain a given energy E is:

$$n = \ln \left(\frac{E}{E_0} \right) / \ln(1 + \epsilon). \quad (10.9)$$

15

$$E_n = E_0(1 + \epsilon)^n \quad (10.8)$$

i.e., the number of cycles needed to a particle to attain a given energy E is:

$$n = \ln \left(\frac{E}{E_0} \right) / \ln(1 + \epsilon). \quad (10.9)$$

On the other hand, at each cycle a particle may escape from the shock region with some probability P_e , which can be considered to be proportional to the velocity V , and then the probability P_{E_n} that a particle escapes from the shock region with an energy greater or equal to E_n is:

$$P_{E_n} = P_e \sum_{j=n}^{\infty} (1 - P_e)^j = (1 - P_e)^n. \quad (10.10)$$

Replacing n by the formula 10.9 one has:

$$P_{E_n} = (1 - P_e)^{\ln \left(\frac{E}{E_0} \right) / \ln(1 + \epsilon)}$$

$$\ln P_{E_n} = \frac{\ln \left(\frac{E}{E_0} \right)}{\ln(1 + \epsilon)} \ln(1 - P_e) = \frac{\ln(1 - P_e)}{\ln(1 + \epsilon)} \ln \left(\frac{E}{E_0} \right).$$

Then

$$\frac{N}{N_0} = P_{E_n} = \left(\frac{E}{E_0} \right)^{-\alpha} \implies \frac{dN}{dE} \propto \left(\frac{E}{E_0} \right)^{-\Gamma} \quad (10.11)$$

with

$$\alpha = -\frac{\ln(1 - P_e)}{\ln(1 + \epsilon)} \simeq \frac{P_e}{\epsilon}; \quad \Gamma = \alpha + 1. \quad (10.12)$$

The 1st order Fermi mechanism predicts then that the energy spectrum is a power law with an almost constant index (both ϵ and P_e are proportional to β).

In the case of the supersonic shock of a monoatomic gas α is predicted by the kinetic theory of gases (see for example the volume on Fluid Mechanics by Landau and Lifshitz) to be around 1 ($\Gamma \sim 2$). The detected spectrum at Earth is steeper. In its long journey from the Galactic sources to the Earth the probability that the particle escapes from the Galaxy is proportional to its energy (see Sect. 10.3.3):

$$\left| \frac{dN}{dE} \right|_{\text{Earth}} \propto \left(\frac{dN}{dE} \right)_{\text{sources}} \times E^{-\delta} \propto \left(\frac{E}{E_0} \right)^{-\Gamma-\delta} \quad (10.13)$$

δ is estimated, in most cosmic rays galactic transport models, to be between 0.3 and 0.6. The 1st order Fermi model provides thus a remarkable agreement with the observed cosmic ray spectrum; however, V has been assumed to be nonrelativistic, and a numerical treatment is needed to account for relativistic speeds.

Note that one can approximate

$$P_e \simeq \frac{T_{\text{cycle}}}{T_e}, \quad (10.14)$$

where T_e is the characteristic time for escape from the acceleration region, and T_{cycle} is the characteristic time for an acceleration cycle. Thus, if E_0 is the typical energy of injection into the accelerator,

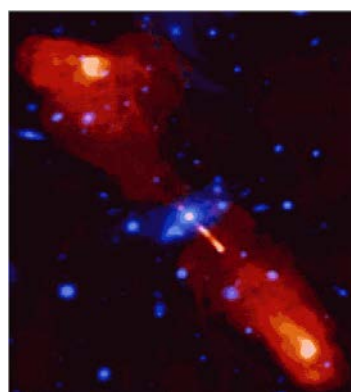
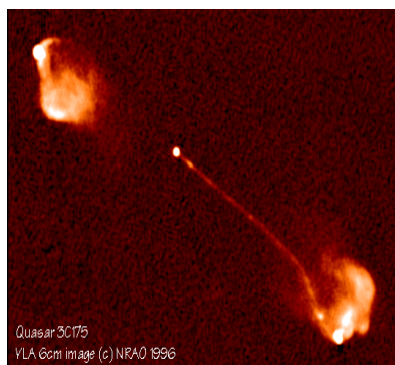
$$E < E_0(1 - \epsilon)^{\tau/T_{\text{cycle}}} \quad (10.15)$$

the maximum energy reachable by an accelerator is constrained by the lifetime τ of the accelerator (typically ~ 1000 years for the active phase of a SNR).

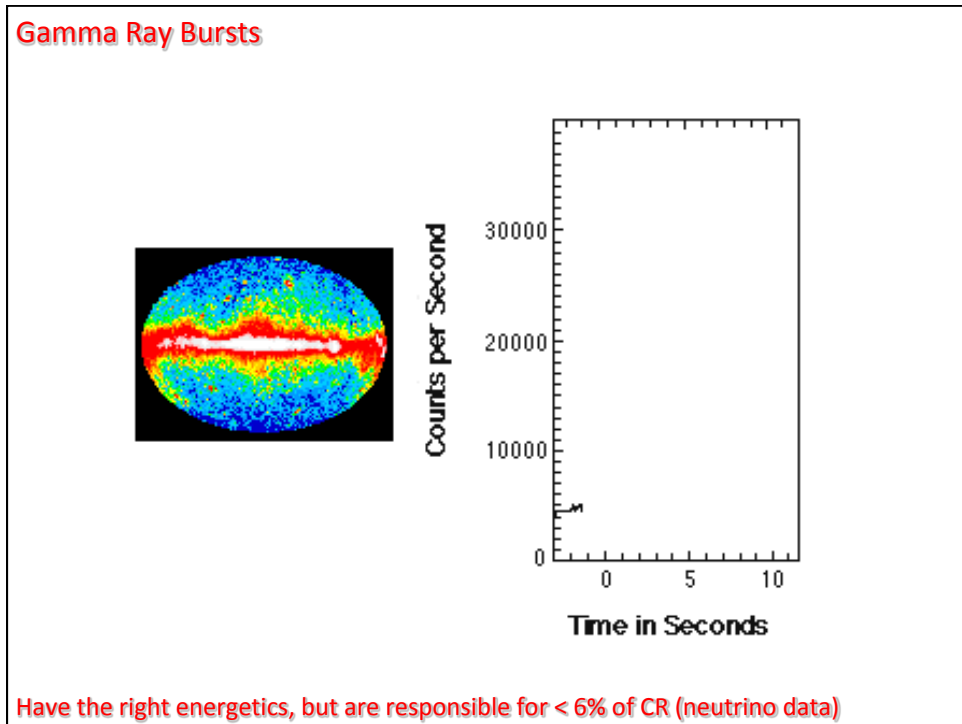
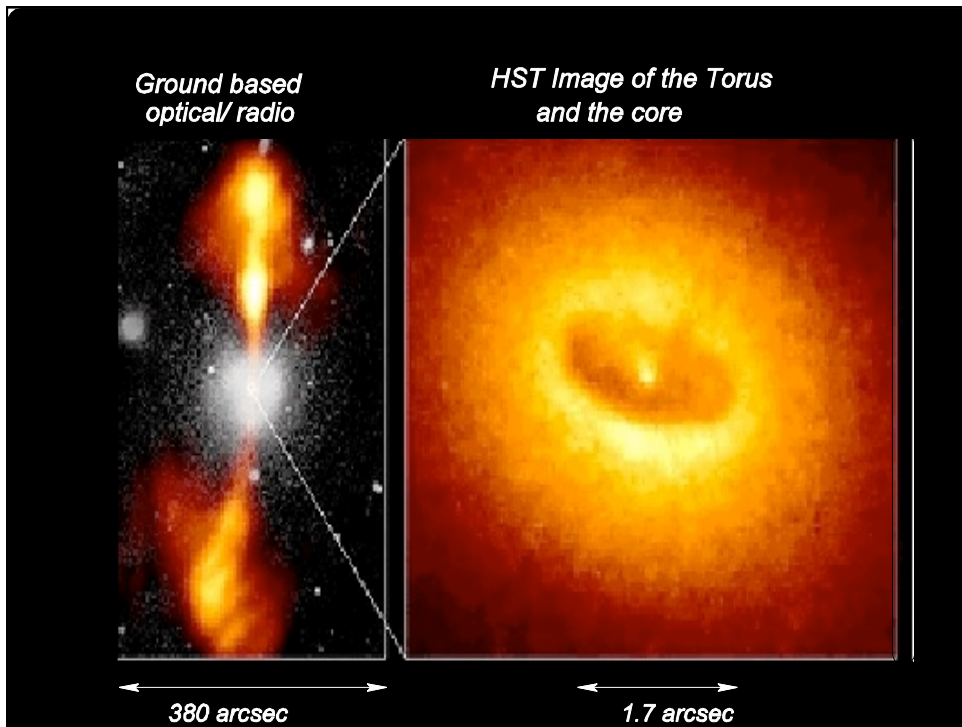
To summarize, the main ingredients of acceleration are magnetic fields and shock waves. These can be present in several types of remnants of gravitational collapses, in particular SNRs, AGN, GRBs. In these objects, clouds of molecular species, dust, photon gas from bremsstrahlung and synchrotron radiation are likely to be present, and accelerated charged particles can interact with them.

Active Galactic Nuclei (AGN)

Central engine accretion disks, jets and hot spots



3C219



Relativistic Shocks: Shock speed approaches c ($V \sim c$)

Main applications in:

- 1) AGN Radio jets
- 2) Gamma-Ray Bursts (fireball, internal shocks, afterglow)

More difficult to understand than **non-relativistic** shocks because:

- Particle speed never \gg shock speed. Cannot use diffusion approximation \rightarrow No simple test-particle power law derivable
- Acceleration, even in test-particle limit, depends critically on scattering properties (i.e., self-gen. B-field), which are unknown
- No direct observations of relativistic shocks. . .
- PIC simulations more difficult to run

Relativistic shocks? \rightarrow Monte Carlo simulations

Analytical solutions vs Numerical Simulations

- Notion of ‘*test particles*’ \rightarrow interact with the plasma shock waves but do not react back to modify the plasma flow.
- Very efficient in describing particle ‘*random walks*’.
- *Random number generation* \rightarrow simulation of the random nature of a physical process.
- Follow closely each particle path using a large number of particles.
- Apply *escape* (momentum and spatial) *boundaries* in the simulation box, according to certain physical conditions.

The study of sources of gamma rays and neutrinos is crucial for high-energy astrophysics: photons and neutrinos point back to their source allowing the identification of high-energy accelerators. Usually the spectrum of photons and neutrinos is measured as the energy flux in erg (or in eV or multiples) per unit area per unit time per unit frequency ν (in Hz), and fitted, where possible, to a power law; the spectral index characterizes the source. Another important quantity is the energy flux νF_ν , usually expressed in erg $\text{cm}^{-2} \text{s}^{-1}$, called the spectral energy distribution (SED). Equivalent formulations use the spectral photon (neutrino) flux dN/dE , and the relation holds:

$$\nu F_\nu = E^2 \frac{dN}{dE}. \quad (10.16)$$

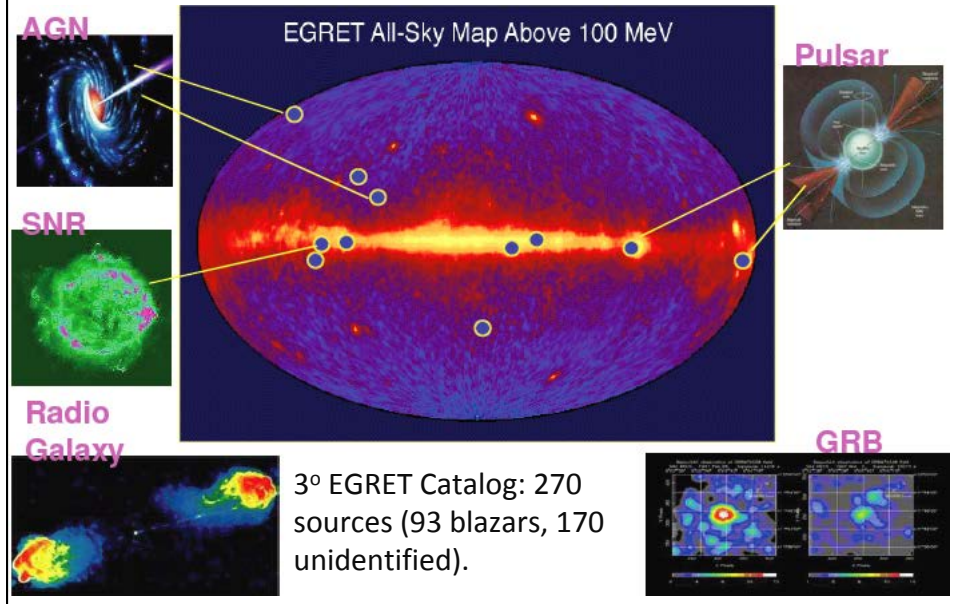
High-energy photons can be produced by radiative and collisional processes, in particular those involving the interaction of high-energy charged particles (for example, electrons, protons, ions accelerated by the shock waves of remnants of gravitational collapses) with nuclear targets such as molecular clouds or radiation fields (magnetic fields, photon fields). We distinguish between purely leptonic mechanisms of production and models in which photons are secondary products of hadronic interactions; the latter provide a direct link between high-energy photon production and the acceleration of charged cosmic rays (Sect. 10.2.5), and produce, in general, also neutrinos. Since neutrinos cannot be practically absorbed nor radiated, and in bottom-up processes they come only through hadronic cascades, the neutrino is a unique tracer of hadronic acceleration.

Positron annihilation and nuclear processes associated with neutron capture and de-excitation of nuclei dominate the gamma-ray production at MeV energies.

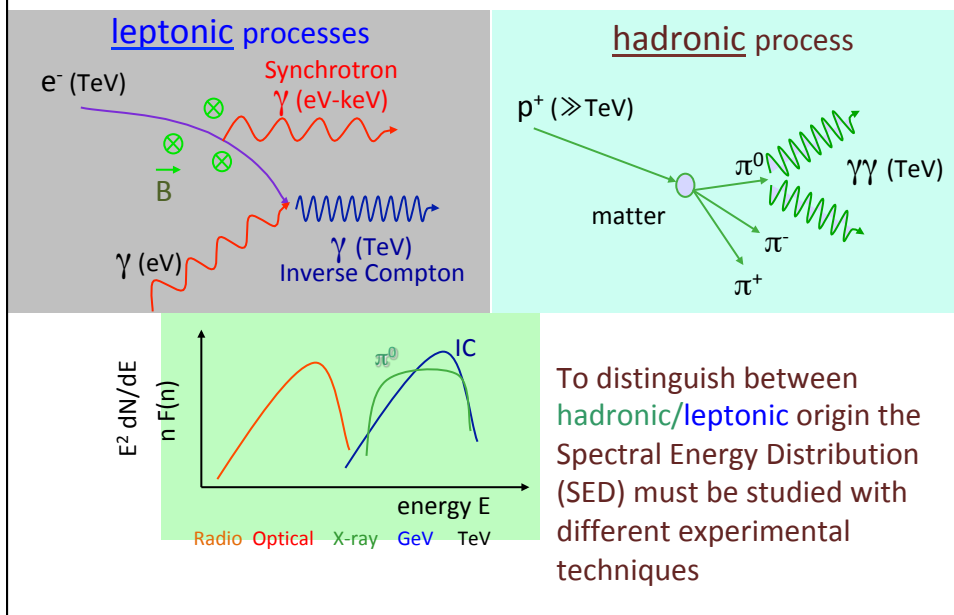
An alternative mechanism (top-down scenario) could be the production via the decay of heavy particles; this mechanism works also for neutrinos.

SOURCES OF GAMMA RAYS RELATION WITH COSMIC RAY PHYSICS

Sources of gamma radiation (and CR?)



Gamma-rays production@sources



Emission models

- Leptonic model (needs B field to generate synchrotron radiation)
- Also hadronic mechanism (needs matter as a target with density > ISM (1p/cm^3), or radiation fields, but cross section is $\sim 1\%$)

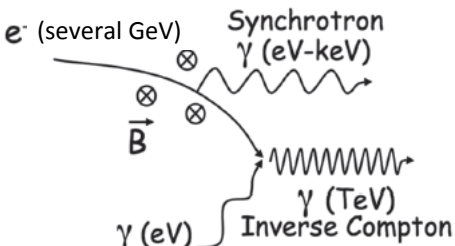
In both cases,

$$\frac{dN_\gamma}{dE_\gamma} \propto \frac{dN_{p,e}}{dE_{p,e}}$$

The key processes: (1) Leptonic

- Synchrotron $P_{\gamma, \text{sync}} \simeq 2.6 \frac{\text{keV}}{\text{s}} \left(\frac{Zm_e}{M} \right)^4 \left(\frac{E}{1 \text{ keV}} \right)^2 \left(\frac{B}{1 \mu\text{G}} \right)^2$

$$\frac{E_{\gamma, \text{sync}}}{1 \text{ eV}} \simeq 0.07 \left(\frac{E_e}{1 \text{ GeV}} \right)^2 \left(\frac{B}{1 \text{ G}} \right) \quad \text{Between IR and X}$$

- Inverse Compton 

since electrons are ultrarelativistic (Lorentz factor 10^{4-5}), the energy of the rescattered photon can be boosted by a large factor.

As we have seen in Chapter 4, the cross section for Compton scattering below a photon energy $m_e c^2$ (the scattered electrons are nonrelativistic) is given by the Thomson cross section $\sigma_T \simeq 665 \text{ mb}$ (Thomson regime), while it rapidly falls off for energy $\gg m_e c^2$ (this is the so-called Klein-Nishina regime).

SSC, the Synchrotron/IC relation

A useful approximate relation linking the electron's energy and the Comptonized photon's energy is:

$$E_{\gamma, \text{IC}} \simeq 6000 \left(\frac{E_e}{1 \text{ GeV}} \right)^2 \left(\frac{\eta}{1 \text{ eV}} \right) \text{ GeV}, \quad (8)$$

and the radiated power is

$$P_{\gamma, \text{IC}} \simeq P_{\gamma, \text{sync}} \frac{U_{\gamma}}{U_B} \propto P_{\gamma, \text{sync}}^2 \quad (9)$$

(in the above expression U_B is the magnetic field energy density and U_{γ} is the photon energy density).

The Compton component can peak at GeV–TeV energies; the two characteristic synchrotron and Compton peaks are clearly visible on top of a general E_{γ}^{-2} dependence. Fig. 2 shows the resulting energy spectrum. This behavior has been verified with high accuracy on the Crab Nebula and on several other emitters, for example on active galactic nuclei. If in a given region the photons from synchrotron radiation can be described by a power law with spectral index p , in the first approximation the tails at the highest energies from both the synchrotron and the Compton mechanisms will have a spectral index p . Note, however, that since the Klein-Nishina cross section is smaller than the Thomson cross section, the Compton scattering becomes less efficient for producing gamma rays at energies larger than ~ 50 TeV.

A key characteristic of the SSC model is a definite correlation between the yields from synchrotron radiation and from IC during a flare (it would be difficult to accommodate in the theory an “orphan flare,” i.e., a flare in the IC region not accompanied by a flare in the synchrotron region). In a first approximation the relation between the power in the IC peak and the power in the synchrotron peak within the purely leptonic SSC model is quadratic. However, there are many hypotheses behind this conclusion; in particular the scattering should be happening with the same population of electrons, in Thompson regime, and the variability would be related exclusively to an increase in the number of electrons.

Flares

$$P_{\gamma, \text{IC}} \simeq P_{\gamma, \text{sync}} \frac{U_{\gamma}}{U_B} \propto P_{\gamma, \text{sync}}^2$$

Real life is more complicated than this, starting with the fact that for VHE photons the scattering can happen in Klein Nishina regime, and with the fact that variability can have many origins and that very probably we see the sum of many components. The correlation is anyway evident in Fig. 3, right for a sample of flares of the near galaxy Markarian 421. Although most of the flaring activities occur almost simultaneously with TeV gamma ray and synchrotron fluxes, observations of 1ES 1959+650 and other AGN have exhibited VHE gamma ray flares without their counterparts in the synchrotron region. The SSC model has been very successful in explaining the SED of AGN, but flares observed in VHE gamma rays with absence of high activity in X-rays are difficult to reconcile with the standard SSC.

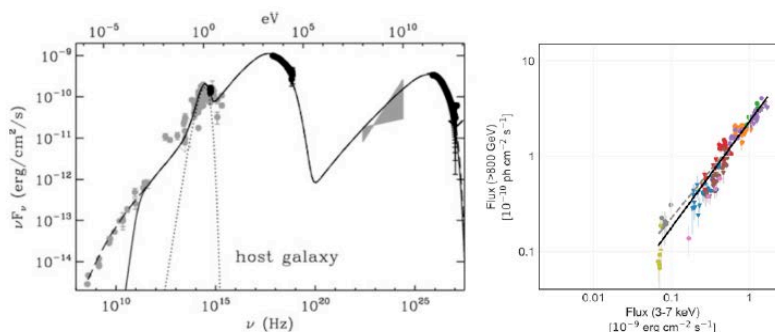


Fig. 3 Left: Typical SED of Markarian 421. Right: Power in the γ -ray band vs. power in the X-ray band for a series of flares in April 2013.

Extension to the continuum

For a power law population of relativistic electrons with a differential spectral index q and a blackbody population of soft photons at a temperature T , mean photon energies and energy distributions can be calculated for electron energies in the Thomson regime and in the relativistic Klein-Nishina regime:

$$\langle E_\gamma \rangle \simeq \frac{4}{3} \gamma_e^2 \langle \eta \rangle \quad \text{for } \gamma_e \eta \ll m_e c^2 \text{ (Thomson limit)} \quad (4)$$

$$\simeq \frac{1}{2} \langle E_e \rangle \quad \text{for } \gamma_e \eta \gg m_e c^2 \text{ (Klein-Nishina limit)} \quad (5)$$

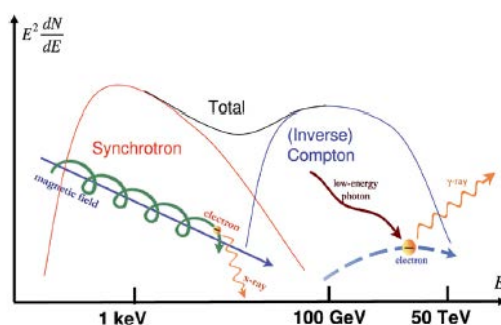
$$\frac{dN_\gamma}{dE_\gamma} \propto E_\gamma^{-\frac{q+1}{2}} \quad \text{for } \gamma_e \eta \ll m_e c^2 \text{ (Thomson limit)} \quad (6)$$

$$\propto E_\gamma^{-(q+1)} \ln(E_\gamma) \quad \text{for } \gamma_e \eta \gg m_e c^2 \text{ (Klein-Nishina limit)} \quad (7)$$

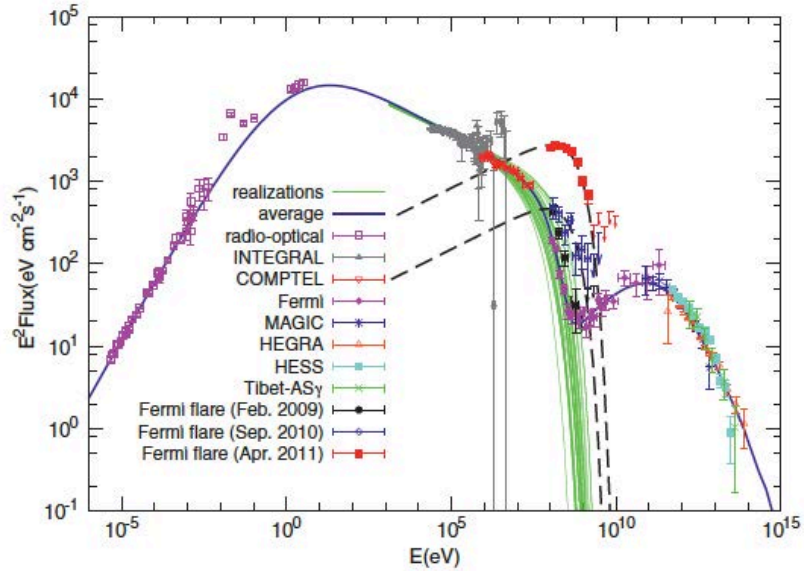
where E_γ denotes the scattered photon's energy, E_e denotes the energy of the parent electron, and η denotes the energy of the seed photon. Note that an observer sees a power-law synchrotron spectrum only if no absorption of photons happens. Sources in which all produced photons are not absorbed are called optically thin. In an optically thick source, significant self-absorption can happen, modifying the shape of the synchrotron spectrum and typically sharpening the cutoff.

Predictions from leptonic models

- Two-humped SED on top of E^{-2}
- In case of flare, full correlation between the increase of the IC peak and the synchrotron peak
- “Orphan” VHE flares difficult to accommodate

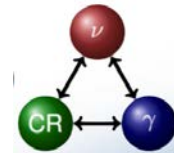
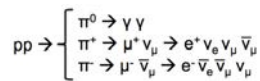


SED of the Crab Nebula

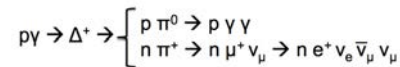


(2) Hadronic

- Proton-hadron



- Photoproduction



$$E_\nu^2 \frac{dN_\nu}{dE_\nu}(E_\nu) \sim \frac{3}{4} K E_\gamma^2 \frac{dN_\gamma}{dE_\gamma}(E_\gamma); K = 1/2 \text{ (2) for } \gamma p \text{ (pp)}$$

- The production rate of γ -rays is not in general the emission rate observed: photons can be absorbed

Hadronic: a look to pA, more in-depth

$$N_\pi \sim 3 \left(\frac{E_p - E_{th}}{\text{GeV}} \right)^{1/4} \sim 3 \left(\frac{E_p}{\text{GeV}} \right)^{1/4}, \quad (10.22)$$

where E_{th} is the threshold energy for pion production, less than 1 GeV - we can neglect it at large proton energies. Consequently, the average pion energy at the source is related to the proton energy, in the direction of flight of the proton, by

$$\langle E_\pi \rangle \sim \frac{1}{3} \left(\frac{E_p}{\text{GeV}} \right)^{3/4},$$

where γ_p is the Lorentz boost of the proton.

The generic pion distribution from the hadronic collision, assuming equipartition of energy among pions, can be written as

$$q_\pi \simeq n_H l \sigma_{pp} \int_{E_{th}}^{\infty} dE_p j_p \left(\frac{E_p}{\text{GeV}} \right)^{3/4} \delta(E_\pi - \langle E_\pi \rangle), \quad (10.23)$$

where n_H is the density of hadrons in the target, l is the depth ($N_H = n_H l$ is the column density), j_p is the proton rate. If the differential proton distribution per energy and time interval at the source is

$$j_p(E_p) = A_p E_p^{-p}, \quad (10.24)$$

making in the integral (10.23) the substitution $E_p \rightarrow E_\pi^{4/3}$ the pion spectrum at the source is

$$q_\pi(E_\pi) \propto E_\pi^{-\frac{4}{3}p + \frac{1}{3}}. \quad (10.25)$$

The photon spectrum is finally

$$q_\gamma(E_\gamma) = A_\gamma E_\gamma^{-\frac{4}{3}p + \frac{1}{3}}, \text{ with } A_\gamma \simeq 800 N_H A_p \sigma_{pp}. \quad (10.26)$$

~300 for neutrinos

Hadronic: a look to $p\gamma$, more in-depth

One can imagine that photoproduction of neutrinos and photons happens mainly via the Δ^+ resonance: $p\gamma \rightarrow N\pi$. The cross sections for the processes $p\gamma \rightarrow p\pi^0$ and $p\gamma \rightarrow n\pi^+$ at the Δ resonance are in the approximate ratio of 2:1, due to isospin balance (Chap. 5). The process happens beyond the threshold energy for producing a Δ^+ :

$$4E_p \epsilon \gtrsim m_\Delta^2, \quad (10.28)$$

where ϵ is the energy of the target photon. The cross section for this reaction peaks at photon energies of about $0.35 m_p c^2$ in the proton rest frame. In the observer's frame the energy ϵ of the target photon is such that $\epsilon E_p \sim 0.35$, with E_p in EeV and ϵ in eV. For UV photons, with a mean energy of 40 eV, this translates into a characteristic proton energy of some 10 PeV.

The photon and neutrino energies are lower than the proton energy by two factors which take into account (i) the average momentum fraction carried by the secondary pions relative to the parent proton² ($\langle x_F \rangle \simeq 0.2$) and (ii) the average fraction of the pion energy carried by the photon in the decay chain $\pi^0 \rightarrow \gamma\gamma$ (1/2) and by the neutrinos in the decay chain $\pi^+ \rightarrow \nu_\mu \mu^+ \rightarrow e^+ \nu_e \bar{\nu}_\mu$ (roughly 3/4 of the pion energy because equal amounts of energy are carried by each lepton). Thus:

$$E_\gamma \sim \frac{E_p}{10}; \quad E_\nu \sim \frac{E_p}{20}. \quad (10.29)$$

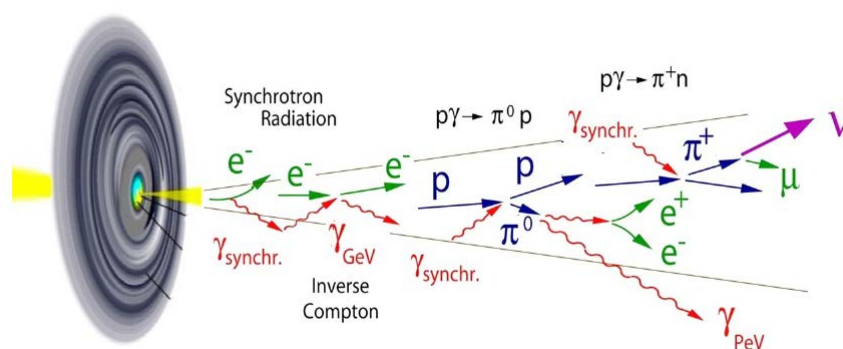
The photon and neutrino spectra are related. All the energy of the π^0 ends up in photons and 3/4 of the π^+ energy goes to neutrinos, which corresponds to a ratio of neutrino to gamma luminosities (L_ν/L_γ)

$$\frac{L_\nu}{L_\gamma} \simeq \frac{3}{8}. \quad (10.30)$$

This ratio is somewhat reduced taking into account that some of the energy of the accelerated protons is lost to direct pair production ($p + \gamma \rightarrow e^+ e^- p$).

If a source is occulted by the presence of thick clouds or material along the line of sight to the Earth, however, gamma rays are absorbed while neutrinos survive.

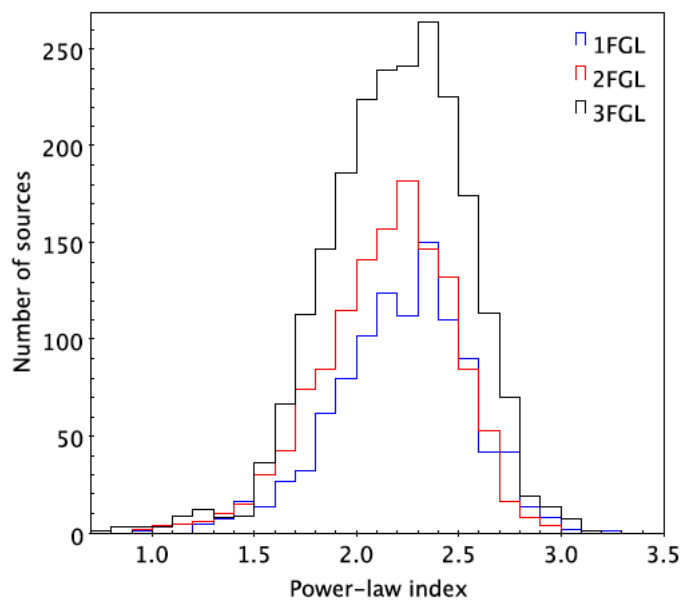
Jets from accretion: relativistic boost



Finally, don't forget top-down mechanisms

- In the GeV-TeV region, γ and ν might come from the decay of heavier particles, or from blobs of energy coming from the annihilation of pairs of particles.
- Experimental data collected up to now do not support the existence of such mechanisms which are anyway searched for actively, especially for photons which are easier to detect, since they might shed light on new physics.
- The top-down mechanism implies also an excess of antimatter: differently from the bottom-up mechanism, which privileges matter with respect to antimatter due to the abundance of the former in the Universe, decays of heavy particles should have approximately the same matter and antimatter content. An excess of antimatter at high energy with respect to what expected by standard production (mostly photon conversions and final states from collisions of CRs with the ISM) is also searched for as a "golden signature" for new particles.
- Some even believe that at the highest energy cosmic rays are the decay products of remnant particles or topological structures created in the early universe.
- Special care is dedicated to the search for products of the decays of particles in the 100-GeV mass range, since this is the order of magnitude of the mass we expect (see the next lecture) for candidate dark matter particles.

High-energy gamma-ray spectral index



SED of several blazars (AGN with jets pointing towards us)

